Effect of end-group sticking energy on the properties of polymer brushes: Comparing experiment and theory

S. Titmuss,[a] W. H. Briscoe, I. E. Dunlop, G. Sakellariou,[b] N. Hadjichristidis,[b] and J. Klein[c]
Physical and Theoretical Chemistry Laboratory, South Parks Road, Oxford OX1 3QZ, United Kingdom

(Received 27 July 2004; accepted 8 September 2004)

Using surface force balance measurements we have established that polystyrene chains bearing three zwitterionic groups have a higher end-group sticking energy than equivalent chains bearing a single zwitterionic group. In a good solvent, polystyrene chains end-functionalized with three zwitterionic groups form brushes of a higher surface coverage than those bearing a single zwitterion. The increase in surface coverage is slow compared with the initial formation of the brush. Measurements of the refractive index allow us to directly quantify the variation of surface coverage, permitting comparison with models for the kinetics of brush formation based on scaling theory and an analytical self-consistent field. We find qualitative support for associating the kinetic barrier with the energy required for an incoming chain to stretch as it penetrates the existing brush. © *2004 American Institute of Physics.* [DOI: 10.1063/1.1811602]

I. INTRODUCTION

At sufficiently high grafting density, chains of a nonadsorbing polymer that are attached at one end to an interface stretch away from the surface forming a *polymer brush*. The presence of the brush layer has been found to significantly modify both normal and shear interactions between brush-bearing surfaces.[1] As a consequence, end-attached polymers have found application in the stabilization of colloidal dispersions and have been suggested to play a role in biolubrication. Various approaches have been adopted to end-attach non-adsorbing chains at interfaces, classified as grafting to or grafting from.[2–4] In the grafting to approach, the nonadsorbing polymer chain is functionalized with either a reactive or adsorbing end-group; grafting from is *in situ* polymerization from a surface initiator.

The systematic variation of the brush height with chain length has been the subject of extensive experimental investigation.[5,6] In particular, the results of Taunton *et al.* have been found to agree well with the predictions of scaling theory.[5,7,8] In addition to chain length, the grafting density should depend on the sticking energy of the end group [see Eq. (5)]. Contrary to this expectation, Kent has commented that although the different approaches to brush formation correspond to widely different (assumed) end-group sticking energies, very similar grafting densities seem to be achieved in all cases.[9]

Most efforts at tailoring brush architecture using the grafting to approach have focussed on the use of diblock copolymers and a selective solvent: the solvent chosen to be good for the nonadsorbing block, termed the tail, and poor for the other, termed the anchor.[6] While technologically relevant, this approach is not ideally suited to a systematic investigation of the variation of brush properties with end-group sticking energy, as interactions between anchor blocks could lead to coverage dependent sticking energies.

We have adopted a different approach using polystyrene chains $[\mathrm{PS}(M)-X_y]$ functionalized at one end by $y=1$, 2, or 3 zwitterionic groups $[X=(\mathrm{CH_3})_2\mathrm{N}^+(\mathrm{CH_2})_3\mathrm{SO_3^-}]$ attached via short (0.5k) polybutadiene spacers (see Table I) in an attempt to control the sticking energy and hence the grafting density.[10] We have previously reported[10] that brushes formed with chains bearing different numbers of zwitterionic sticking groups do not appear to show a systematic variation in brush properties; here we present a resolution of this unexpected observation.

In particular, we establish that increasing the number of zwitterionic groups does increase the sticking energy and that this does result in an increase in the grafting density. We find that the increase in the grafting density follows a logarithmic time dependence with a time scale that is long compared with the construction time of brushes formed from chains bearing a single zwitterionic sticking group.[5]

The paper is structured as follows: In the following section we present scaling relations for the dependence of grafting density and brush height on the end-group sticking energy at equilibrium; after outlining the experimental procedure we present the results of two types of experiment; in the first we demonstrate that chains bearing three zwitterions will displace shorter chains bearing a single zwitterion, establishing that increasing the number of zwitterions *does* increase the end-group sticking energy; we then follow the kinetics of the growth of a $\mathrm{PS}(65)-X_3$ brush over a timescale that is *long* compared with the formation of brushes bearing a single zwitterion; the experimental kinetics are compared with a model developed in the Appendix; we also use the scaling relations presented in the text to *predict* the equilibrium properties of the growing $\mathrm{PS}(65)-X_3$ brush

[a]Electronic mail: simon.titmuss@chem.ox.ac.uk
[b]Department of Chemistry, University of Athens, Greece.
[c]Also at Weizmann Institute of Science, Rehovot, Israel. Electronic mail: jacob.klein@chem.ox.ac.uk

TABLE I. Molecular properties of the polymers PS(M)$-X_y$ used in this study.

Polymer	M_w	M_w/M_n	wt % polybutadiene	R_F (nm)
PS(25)$-X$	26 000	1.04	⋯	12.2
PS(25)$-X_3$	28 000	1.04	4.5	12.2
PS(65)$-X_3$	67 000	1.05	1.8	21.1

from the directly measured properties (height and coverage) of an equilibrium brush constructed from shorter chains bearing a single zwitterion (PS(25)-X).

II. SCALING PREDICTIONS: GRAFTING DENSITY AND BRUSH HEIGHT

The chain configuration in a brush is very different from that of a free coil in solution: in a good solvent, the chain is stretched to minimize the osmotic segment-segment interaction. Using a scaling approach, Alexander found that the segment-segment repulsion is balanced by the loss of chain entropy, due to stretching, for a brush height,

$$L_0 \sim Na(a^2\sigma)^{1/3} \sim Na^{5/3}s^{-2/3}, \tag{1}$$

where N is the degree of polymerization, a the Kuhn segment length, and $\sigma = 1/s^2$ is the surface coverage (chains/unit area) of chains with average spacing s.[7,8]

We follow the scaling approach, originally given by Alexander[7] and outlined by Kumacheva *et al.*,[11] to determine how the grafting density depends on the chain length and the sticking energy of the end group.

The brush is regarded to comprise close-packed blobs: there are three contributions to the free energy f of a molecule in a brush,

$$f \cong [-\Delta + n_b + \ln(a^2\sigma)]k_BT, \tag{2}$$

respectively, the sticking energy, the excess repulsive energy (where n_b is the number of blobs) and the surface entropy term. For a brush comprising n chains, covering an area $\mathcal{A} = ns^2$, the total free energy of the brush, $\mathcal{F}_{\text{brush}} = nf$. Blobs are regarded as repulsive spheres containing g monomers, hence $n_b = N/g$ and the blob size $s = g^{3/5}a$; each blob costs a free energy k_BT. In equilibrium, the chemical potential of a chain in the brush $[\mu_{\text{brush}} = (\partial \mathcal{F}_{\text{brush}}/\partial n)_{\mathcal{A}}]$ must equal the chemical potential of a chain in the reservoir ($\mu_{\text{ch}} \cong k_BT \ln \phi_b$, for volume fraction ϕ_b) and the area occupied by a chain in the brush:[11]

$$s^2 \cong a^2 \left\{ \frac{(11/6)N}{\Delta + \ln[\phi_b/(a^2\sigma)]} \right\}^{6/5}. \tag{3}$$

Neglecting the contribution to Eq. (3) due to the difference in mixing entropy for surface and bulk chains allows simple scaling dependencies to be derived for the area per chain and brush height that are the same as those obtained by our earlier approach,[10]

$$s^2 \sim a^2 \left[\frac{N}{\Delta} \right]^{6/5} \tag{4}$$

and

$$L_0 \sim aN^{3/5}\Delta^{2/5}. \tag{5}$$

The scaling treatment clearly predicts a strong variation in the *equilibrium* brush height with the end-group sticking energy that was not observed in our previous study.[10]

It is interesting to compare the form of the adsorption isotherm implied by Eq. (3),

$$\phi_b = (a^2\sigma)\exp[-\Delta + (6/11)N(a^2\sigma)^{5/6}] \tag{6}$$

with Eq. (A6) derived in the appendix by following the self-consistent field (SCF) approach of Ligoure and Leibler,[12] using a slightly modified form for the chemical potentials of chains in the brush and bulk, which allows easy comparison with experimental data.

In both cases, the second term in the exponential is the chemical potential of the chain in the brush environment. As pointed out by Alexander,[7] this is equivalent to the free energy change due to the confinement of the chain to a cylinder of cross-sectional area σ^{-1}. Hence the surface coverage is determined by the net energetic stabilization of a tethered chain compared to a chain in the bulk.

III. EXPERIMENT

We use the surface force balance (SFB) technique, described in detail previously,[13,14] to measure the interaction force $F_n(D)$ as a function of separation D between mica surfaces bearing the end-attached polymer layers. The separation between the surfaces is measured interferometrically, with an accuracy of ca. 0.3 nm, permitting the measurement of normal forces with a resolution of order 100 nN. The apparatus also has the capability to measure lateral forces with similar sensitivity, although we do not exploit this in the current study. The optical technique also allows the refractive index of the medium between the mica surfaces to be measured, permitting a direct measure of the amount of surface-attached polymer.

The mica pieces (ASTM V-2, Muscovite mica, S & J Trading, New York) used in these experiments were typically 2–4 μm thick. A hot platinum wire (diameter 0.125 mm) was only used to cut a large piece (ca. 10 cm^2) of uniform thickness, with no cuts made upstream of the mica in the laminar flow hood; a scalpel was used to divide this piece into the smaller samples (ca. 1 cm^2) used in the experiments. The mica pieces are coated with a ca. 50 nm thick silver film and mounted, silver-side down, across cylindrical lenses using glucose (AR grade, Fluka) as a glue.

After mounting, the clean mica surfaces were brought to a separation from which a spontaneous jump into contact, under the action of the van der Waals attraction, was observed in air, establishing the zero of surface separation, relative to which all subsequent separation measurements are made. Pure toluene (AR grade, dried over 4A molecular sieves, Fluka) was then introduced between the surfaces and the forces measured in the absence of polymer. The surfaces were then separated to ca. 500 μm; ca. 5 ml of toluene was removed and replaced by an equal volume of the polymer solution; thorough mixing was ensured by using the syringe to cycle ca. 2 ml in and out of the incubating bath. In the case of the *displacement* experiments described below, the

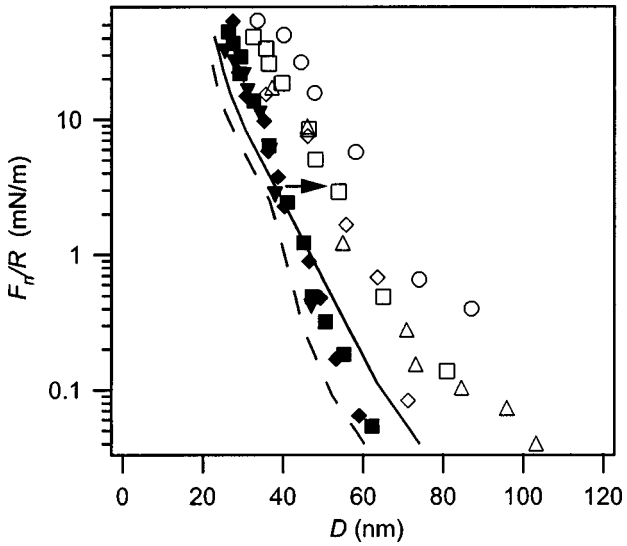

FIG. 1. Force-distance profiles measured between (a) surfaces bearing a PS(25)$-X$ brush (filled symbols) and (b) the same surfaces, following incubation in a solution of PS(65)$-X_3$ for 80 h (empty symbols). The solid line indicates the interaction measured after 20 h incubation in PS(65)$-X_3$. The dashed line is taken from Ref. 16. Notice that the range of interaction measured in this work is greater by 5 nm. We attribute this to a higher surface coverage resulting from the exclusion of water and the longer incubation time.

same procedure was followed for the subsequent introduction of different polymers. The chamber was loaded with a small quantity of phosphorus pentoxide as a drying agent.

The molecular characteristics of the polymers used in this study are summarized in Table I and a description of the synthetic procedure can be found elsewhere.[10]

The force profiles presented in Figs. 1–3 have been normalized by the measured radius of curvature of the mounted mica ($R \approx 0.01$ m). Within the Derjaguin approximation, $F_n(D)/R = 2\pi E(D)$, where $E(D)$ is the equivalent interaction free energy per unit area for parallel plates.

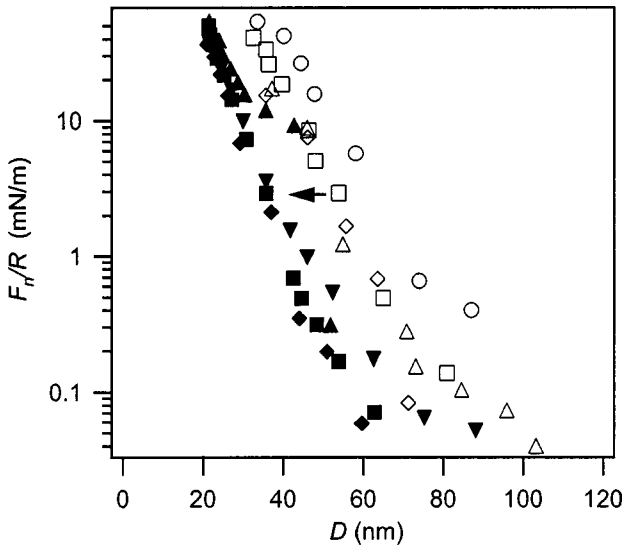

FIG. 2. Force-distance profile measured between the same surfaces as in Fig. 1: empty symbols identical to Fig. 1, filled symbols following incubation in a solution of PS(25)$-X_3$ for 40 h.

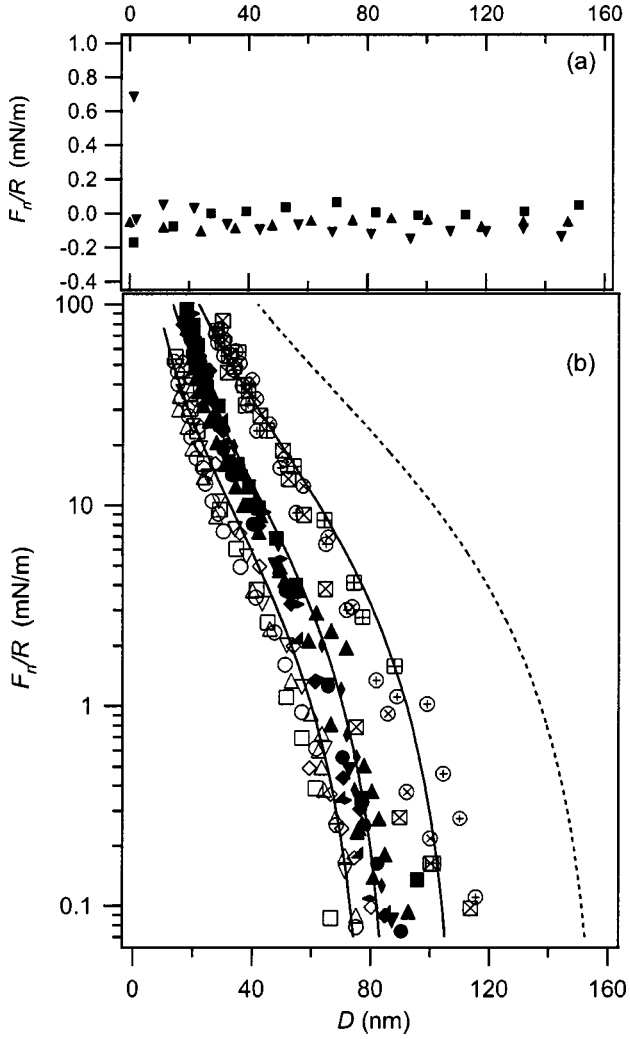

FIG. 3. (a) Force-distance profiles measured across toluene before introducing PS$-X$. (b) Force distance profiles measured, between the same surfaces, as a function of incubation time after introducing PS(65)$-X_3$. Empty symbols correspond to an incubation time of 3–14 h, filled symbols correspond to an incubation time of 40–60 h and crossed symbols correspond to an incubation time of 136–150 h. The solid lines are the fits to Alexander-de Gennes force profiles [Eq. (8)] that yield the parameters listed in Table II. The dashed line is a prediction of the equilibrium Alexander-de Gennes force profile for PS(65)$-X_3$ assuming chain spacing $s = 4.0$ nm and $L_0 = 79$ nm, which are estimated from the values for the PS(25)$-X$ brush using the scaling relations derived in the text.

IV. RESULTS AND DISCUSSION

In all experiments, before introducing PS$-X$, normal $F_n(D)$ profiles were measured between bare mica surfaces immersed in pure toluene. Some of the resulting profiles are shown in the upper panel in Fig. 3. No forces were measured for $D > 3$ nm and the surfaces came into an adhesive contact at $D = 1 \pm 1$ nm. The scatter in the magnitude of the force at closest approach, and indeed the distance of closest approach, are suggestive of the structural forces that have been observed across similar nonpolar liquids;[15] the precise form of such forces is not relevant to the subsequent investigation of end-attached polymers and was not determined in the present study. Furthermore, the measured contact adhesion, $F_{ad}/R = (-65 \pm 5)$ mN/m, is comparable to the largest values measured by Christenson between mica surfaces in inti-

mate contact in benzene and cyclohexane.[15] The key point is that, in all the experiments reported here, the adhesion and absence of long range forces indicated the system to be free from contamination before introducing PS–X.

We report the findings of two types of experiment: in the first we use the chain length and end-group sticking energy to control the free energy of chains in brush environment; in the second we follow the kinetics of brush growth.

A. Sticking energy of three zwiterion end group

The first of these experiments allows us to clearly establish that increasing the number of zwitterionic groups from one to three does result in an increase in the end-group sticking energy. In an earlier pair of experiments, it was established that for PS(M)-X with the same end group, shorter chains will displace longer chains.[11,16] The driving force is the greater free energy cost to the longer chain when confined in the tube like environment of a brush. They derive a simple expression for the interfacial free energy (for a unit area),

$$\Delta F(\Delta,N)\cong(k_BT/a^2)[\{\Delta+\ln[\phi_b/(a^2\sigma)]\}/N]^{6/5}\ln\phi_b. \quad (7)$$

It is clear that for constant sticking energy Δ, the interfacial energy is more favorable for shorter chains. Equation (7) suggests that it may be possible for long chains (with a high end-group sticking energy) to displace short chains (with a lower end-group sticking energy).

The force profiles presented in Figs. 1 and 2 demonstrate a test of this suggestion. The filled symbols in Fig. 1 correspond to the interaction force profile measured between brushes formed by the incubation of bare mica surfaces in PS(25)–X ($\phi_b=1\times10^{-4}$) for 15 h; the empty symbols correspond to the limiting interaction measured following the introduction of PS(65)–X_3 and incubation for periods between 85 and 133 h $\{\phi_b[\mathrm{PS}(25)\text{–}X]=5\times10^{-5}/\phi_b[\mathrm{PS}(65)\text{–}X_3]=1.8\times10^{-4}\}$. The increase in the range of the interaction provides clear evidence that the longer chain (three zwitterionic groups) has clearly invaded the brush formed from the shorter chains (single zwitterionic group), displacing the shorter chains. Following the argument given above, this could only happen if the increased number of zwitterionic groups does *increase* the sticking energy of the end group. Furthermore, we can estimate, from Eq. (7), that the the sticking energy of the invading PS(65)–X_3 must be at least 2.6 times (the ratio of the degrees of polymerization, 65/25) greater than the sticking energy of PS(25)–X. In Fig. 1, we present only the limiting data after a long incubation period (minimum of 85 h), with no significant change being observed after a further 48 h incubation. We note that there is greater variation between profiles measured over this limiting period than for the initial PS(25)–X brushes, or is typical for our measurements of equilibrium brushes; this could be an indication that the system has not reached equilibrium. Measurements made at intermediate times lay between these limiting profiles and the first profile measured after 20 h incubation, indicated by the solid line in Fig. 1. These intermediate profiles also showed greater variation between force profiles than is apparent in the PS(25)–X profile. This could be an indication of a mixed PS(25)–X/PS(65)–X_3 brush.

Figure 2 shows the result of incubating the limiting brush formed by the displacement of PS(25)–X by PS(65)–X_3 in a solution of PS(25)–X_3 for a further 40 h. The open symbols again correspond to the PS(65)–X_3, while the filled symbols correspond to PS(25)–X_3. It is clear that when the chains have the *same* end group, the shorter chains displace the longer chains, as earlier observed.[11,16] The time scale for this displacement (ca. 40 h) is significantly longer than that observed in the earlier PS–X experiments[11,16] (ca. 2 h). This is consistent with the hypothesis that increasing the number of sticking groups has increased the sticking energy: for a chain to be displaced it now has to desorb from a deeper potential well.

These observations provide clear evidence that increasing the number of zwitterionic groups does increase the sticking energy of the end group. The time scale for the displacement of the the shorter chain (lower end-group sticking energy) by the longer chain (higher end-group sticking energy) appears to be slower than the displacement of longer chains by shorter chains (with equivalent end-groups) observed by Klein and Kumacheva.[11,16] In the latter case, the correlation length of the long chain brush is much larger than the coil size of the invading shorter chain, hence the existing brush does not present a significant potential barrier. Conversely, in the case reported here, the longer invading chain has to penetrate pores much smaller than its free coil size if it is to invade the short chain brush. The short chain brush may thus present a significant potential barrier to the invading longer chain.

B. Evolution of PS(65)–X_3 brush: Brush properties

In the second set of experiments we investigate the kinetics of PS(65)–X_3 brush formation onto a bare mica surface. The lower panel of Fig. 3 shows the variation in the force-distance profiles for interactions between mica surfaces bearing PS(65)–X_3 as a function of incubation time. The data points correspond to a large number of profiles measured both on compression and decompression. In line with previous measurements of PS–X brushes,[5] there is no systematic difference between profiles measured on compression and decompression. There is, however, a systematic variation with increasing incubation time; this is in contrast to the behavior observed with chains bearing a single zwitterionic group, for which an incubation period of 2–3 h was found to be sufficient to achieve the equilibrium coverage.[5] The data sets correspond to three different incubation periods: 3–14 h, 40–60 h, and 136–150 h. There is no *systematic* variation between profiles recorded in any one time frame, while there is clearly a systematic variation in the range and magnitude of the profiles measured in different time frames. Each of the time frames corresponds to periods in which force profiles were being measured, during which the surface separation was ca. 500 nm or less. During the intervening periods, the surfaces were separated to ca. 500 μm to allow for equilibration with the bulk solution; we consider these intervening periods to increment the incubation time. The force profiles measured in the first time frame

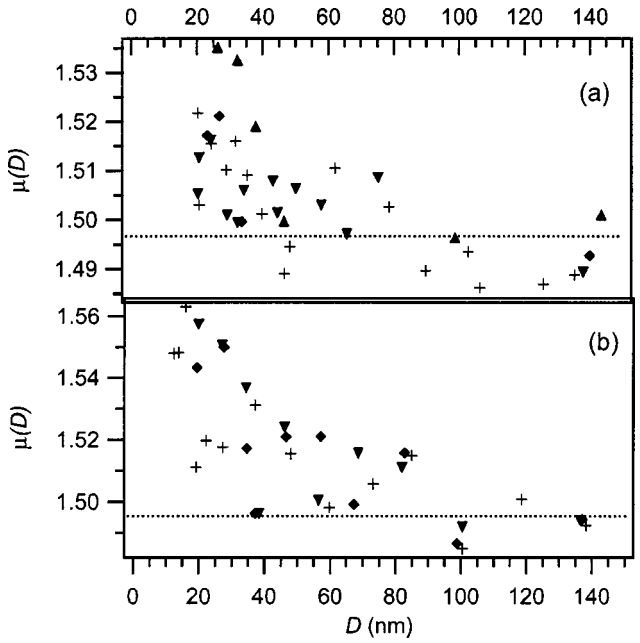

FIG. 4. (a) Refractive index $\mu(D)$ as a function of separation between mica surfaces bearing PS(25)$-X$ brushes; force profiles measured at the same time are not shown but were identical to those shown by filled symbols in Fig. 1. (b) Refractive index as a function of separation between mica surfaces that have been incubated in PS(65)$-X_3$ for 50 h, corresponding to the force profiles indicated by filled symbols in Fig. 3 (b). In both cases the refractive index of pure toluene is indicated by the dotted line at $\mu_{\text{tol}} = 1.497$.

are identical to those presented in our earlier study[10] in which comparatively short incubation times were employed.

To quantify the variation in the surface coverage, we use the refractive index profiles measured in the second time frame, shown in Fig. 4(b), to provide an absolute measure of the surface coverage at this stage.[14,17] Assuming that the refractive index depends linearly on the volume fraction of surface bound polymer, and assuming the surface coverage Γ to be independent of separation[18] we find an adsorbed amount of (5.7 ± 1.8) mg/m^2 corresponding to a mean chain spacing, $s = (4.5 \pm 0.9)$ nm.

We did not measure refractive index profiles for 3–14 h, or for 136 h. Instead we adopt two procedures to determine the coverage during these periods from the directly measured value in the 40–60 h period. The first procedure involves fitting the measured force profiles to Eq. (8), which is obtained by integrating the Alexander–de Gennes expression[8] for the force/unit area acting on parallel plates bearing brushes of uncompressed height L_0:

$$E(D) = \frac{F(D)}{2\pi R} = \frac{2L_0 k_B T}{s^3}\left[\frac{4c_1}{5}\left(\frac{2L_0}{D}\right)^{5/4} + \frac{4c_2}{7}\left(\frac{D}{2L_0}\right)^{7/4} - \left(\frac{4c_1}{5} + \frac{4c_2}{7}\right)\right], \tag{8}$$

where the first term represents the increasing segment-segment (osmotic) repulsion and the second the increase in the chain entropy, as the chain stretching decreases with increasing compression. Although c_1 and c_2 are in principle different constants of order unity, in the fitting procedure that follows we assume them to be the same. The justification is that the fit is dominated by the high compression region which is dominated by the osmotic term, described by c_1. To use this expression the scaling constant must be determined: fixing $s = 4.5$ nm [from refractive index profile in Fig. 4 (b)] and the uncompressed brush height $L_0 = 44$ nm (from the onset distance of the repulsion) and using Eq. (8) to fit the force profiles measured at the same time as the refractive index profiles (filled symbols in Fig. 3 yields the constant $c \cong 0.5$). Having evaluated this constant fitting the profiles for 3–14 h and 136 h, for which only L_0 is known, determines the corresponding values for the mean chain spacing s. The resulting parameters that describe the development of the brush are given in Table II. Table II also lists the number of blobs in the uncompressed brush, $n_{\text{blobs}} \cong L_0/s$, in the three phases of the brush development.

The second approach to obtain the surface coverages for the initial (3–14 h) and final (136 h) incubation periods follows that outlined by Taunton *et al.*[5] Focusing on the high compression region of the profiles, dominated by osmotic segment-segment repulsions, which are treated using a Flory-Huggins mean-field approximation for the osmotic pressure,[19] the interaction energy at a separation D' is given by

$$E(D') = \int_{2L_0}^{D'} \Pi(\phi(D))dD = \text{const} \times (M^2/D's^4), \tag{9}$$

so, for a given $E(D')$ (corresponding to $F_n/R = 10$ mN/m in this case),

$$s^2 = \text{const} \times (M/D'^{1/2}). \tag{10}$$

Following this approach to obtain s for time frames 1 ($D' = 29$ nm) and 3 ($D' = 55$ nm) from the directly measured

TABLE II. Brush parameters derived from fitting experimental force profiles measured for PS(65)$-X_3$ to Alexander–de Gennes force profiles. Figures in brackets obtained using the alternative procedure of comparing the interaction free energy in the high compression regime via a Flory-Huggins mean-field scaling expression. The table also shows the corresponding surface coverages (chains/nm^2) and the fractional coverage expressed relative to an equilibrium coverage of $\sigma_{eq} = 0.0625$ nm^{-2} estimated by applying a scaling approach to the directly measured surface coverage of the equilibrium PS(25)$-X$ brush (see text for details).

Incubation time (h)	L_0 (nm)	s (nm)	$\sigma(t)$ (nm^{-2})	$\theta = \sigma(t)/\sigma_{eq}$	n_{blobs}
3–14	40 ± 1	5.2 (4.9)	0.042	0.67	7.7
40–60	44 ± 1	4.5 ± 0.9	0.049	0.79	9.8
136	55 ± 1	4.3 (4.2)	0.057	0.91	12.8

chain spacing of time frame 2, yields 4.9 nm and 4.2 nm, respectively, as indicated (in parentheses) in Table II; these values are within the scatter of the values obtained from our refractive index measurements. In our analysis of the kinetics of brush formation we use the estimates of interanchor separation obtained directly from the refractive index profile (time frame 2) and the mean-field comparison of the high compression region (time frames 1 and 3) to provide a measure of the surface coverage.

It is clear from the variation in the force profiles in Fig. 3 that the PS(65)$-X_3$ brush is developing during the course of the measurements. We use a scaling theory approach to predict the equilibrium properties of this brush and hence characterize how far the growing brush is from equilibrium. Our starting point is the interaction force profile measured between surfaces bearing what we believe to be fully developed PS(25)$-X$ brushes. The solid symbols in Fig. 1 show force profiles measured between mica surfaces that have been incubated in solutions of PS(25)$-X$ ($\phi_b \sim 1\times10^{-4}$) for a period of 20 h; profiles measured in separate experiments (different mica substrates) with shorter incubation periods were identical but are not shown. The onset of the interaction can be identified as $L_0=(29\pm3)$ nm. From the corresponding refractive index profile, shown in Fig. 4(a), we determine a surface coverage of (3.1 ± 1.6) mg/m^2, equivalent to a chain spacing of $s=(4.4\pm1.5)$ nm. Using Eqs. (4) and (5), we predict an equilibrium chain spacing and brush height for the PS(65)$-X_3$ brush of $s=(4.0\pm1.6)$ nm and $L_0=(79\pm8)$ nm, respectively. The predicted force profile for such a brush obtained using these values of s and L_0 in Eq. (8) is shown by the dashed line on Fig. 3(b). We use the value of the equilibrium surface coverage evaluated in this way ($\sigma_{eq}=0.06$ chains/nm^2) to express the surface coverages determined from the refractive index and the Flory-Huggins mean-field procedure (bracketed figures) as fractional surface coverages ($\theta=\sigma/\sigma_{eq}$); these fractional coverages are also shown in Table II.

C. Evolution of PS(65)$-X_3$ brush: Kinetic models

The kinetics of brush formation has been the subject of both theoretical[12,20–25] and experimental[26–33] investigations. With the exception of Pelletier *et al.*,[32] the effect of the kinetics of brush formation on the interactions between brush bearing surfaces has not been considered. In the original PS$-X$ experiments of Taunton *et al.*,[5] it was noted that saturation coverage was achieved on a time scale of 2–3 h. From the data presented in Table II and Fig. 5, it is clear that the time to reach saturation is substantially longer in the case of a PS(65)$-X_3$ brush. A possible explanation is afforded by a consideration of Eqs. (4) and (5) and the schematic representation in Fig. 5. Scaling arguments [Eq. (4)] predict that the equilibrium coverage for the PS$-X_3$ brush should be $3^{6/5}$ times that for a PS$-X$ brush with the same chain length (assuming sticking energy due to three zwitterions is three times that due to a single zwitterion), hence the equilibrium chain spacing should be about half that for the PS$-X$ brush. Consequently, chains arriving at a surface bearing an equilibrium PS$-X_3$ brush have to penetrate a tube with half the

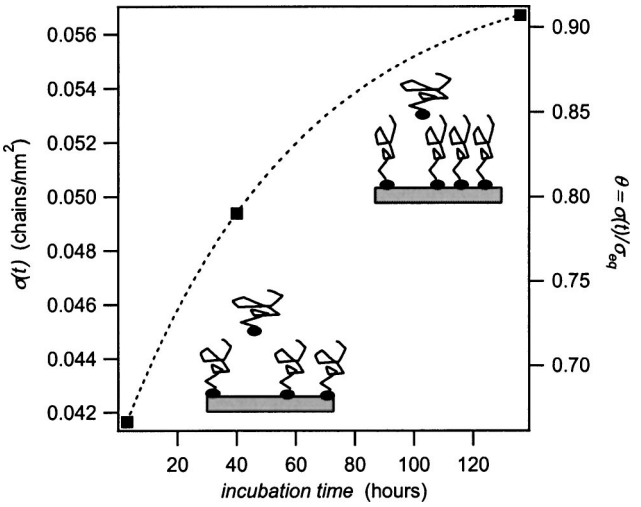

FIG. 5. Experimentally determined surface coverage of PS(65)$-X_3$ as a function of the incubation time. The fractional coverage $\theta=\sigma/\sigma_{eq}$, where $\sigma_{eq}=0.0625$ chains/m^2 is estimated by applying scaling arguments to a direct measurement of the equilibrium surface coverage of a PS(25)$-X$ brush. The line is an exponential fit that is intended to guide the eye. The inset is a cartoon to illustrate the confinement induced origin of the greater potential barrier faced by chains penetrating denser brushes.

diameter of chains arriving at an equilibrium PS$-X$ brush. Confinement of a polymer chain to a tube costs free energy, hence we expect the denser brush to present a larger potential barrier for the chains that arrive as equilibrium is approached. This picture is consistent with the findings of the detailed kinetic investigations[26–28,30,31] which use optical methods (surface plasmon resonance and ellipsometry), radiolabeling or neutron reflectivity to follow the surface excess as a function of time and find a rapid diffusion-limited regime followed by a slower regime. The first regime is thought to end when the surface attached tails start to overlap and stretch out from the surface. We will show below that the time scale for the second regime depends strongly on the density of the growing brush and hence on the sticking energy of the end group. Most of the kinetic studies have employed diblock copolymers and selective solvents to form brushes. This architecture complicates the investigation of the kinetics of brush formation, as it is possible that the sticking energy varies as a function of coverage and that there are additional structural rearrangements occurring within the layer formed by the sticky block.[34] We can, however, comment that the time scale for the formation of brush of similar length PS chains (with poly(2-vinylpyridine) anchoring block) followed by Pelletier *et al.*[32] is similar to that found in this study. Kinetic studies employing nonpolymeric anchoring points (such as in this work) are less numerous. Clarke *et al.* observe a similar time scale for the development of a brush comprising PS chains of a similar length bearing a carboxylic acid sticking group, from a melt of much longer PS homopolymer chains.[27] Despite using much shorter thiolated poly(ethylene glycol), Himmelhaus *et al.* find that brush growth extends over a period of tens of hours;[29] the key factor is the very high grafting density that the high sticking energy of the thiol affords.

The evolution of dense brushes on a time scale that is

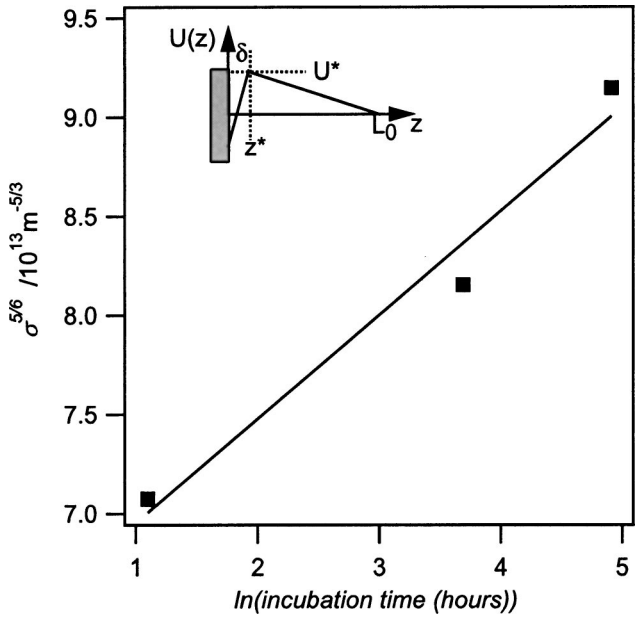

FIG. 6. Experimentally determined surface coverage as a function of the incubation time, plotted to test the scaling description of the kinetics of brush formation. The line of best fit is consistent with $N=320$. The inset shows the scaling form of the chemical potential of a chain in the brush environment.

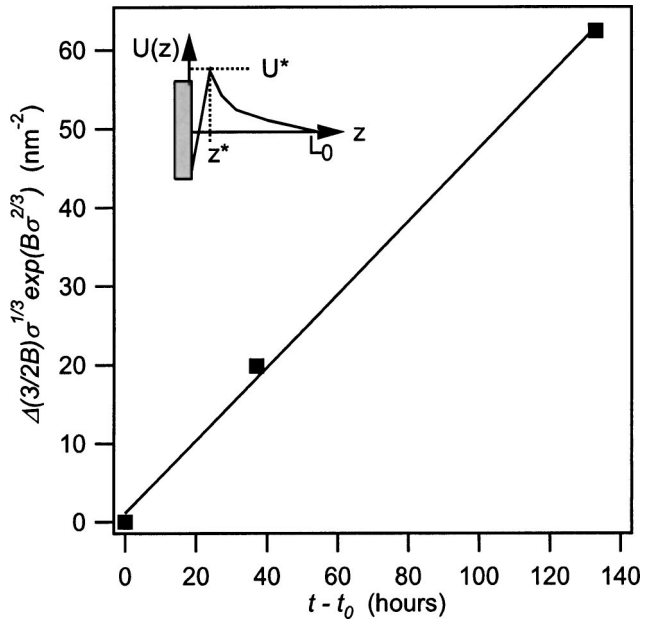

FIG. 7. Experimentally determined surface coverage relative to the coverage measured in the first time frame as a function of additional incubation time. The inset shows the SCF form of the chemical potential of a chain in the brush environment.

long compared with the diffusion-limited build up of mushrooms and moderately stretched brushes has been predicted by a number of analytical theories[12,20,21,35] that can be traced back to Halperin and Alexander.[36] At the heart of these theories is the idea that for a chain to enter a brush, it has to penetrate a confining tube, which results in a potential barrier, and that the penetration occurs by a reptative motion. In the Appendix, we develop a framework, based on these analytical models, to allow us to examine the effect that the model for the potential has on the comparison with the experimentally observed kinetics.

Assuming a scaling form for the position-dependent chemical potential of an incoming chain in the brush environment (shown as inset to Fig. 6), predicts an increase in the surface coverage that is approximately logarithmic with time [Eq. (B11)]:

$$(\sigma a^2)^{5/6}=\mathcal{C}+N^{-1}\ln\left|\frac{t}{\tau}\right|, \tag{11}$$

where $\tau=6\pi\eta/c_0k_BT$ is the characteristic time for brush growth. In Fig. 6 we plot $\sigma^{5/6}$ as a function of $\ln t$, where t is the incubation time in hours, using $\sigma=1/s^2$, where s is the average chain spacing obtained from the refractive index data [Fig. 4(b)] and a mean-field comparison of the high compression region (10 mN/m) of the force profiles in Fig. 3(b). Equation (11) predicts a straight line with gradient $(Na^{5/3})^{-1}$. Using $a=0.76$ nm and the experimentally determined gradient of 5×10^{12} m$^{-5/3}$ yields $N\sim320$, compared with the true degree of polymerization of $N=625$. It is important to appreciate that the free energy barrier in Eq. (B9) is correct to within a scaling constant of order unity, so we do not feel that it is appropriate to attach too much significance to the gradient of Fig. 6.

To examine the effect that changing to a SCF description of the potential barrier (shown schematically as the inset to Fig. 7) has on the comparison with our experimental data we use Eq. (B20) which gives the evolution of surface coverage $\sigma(t)$ relative to the coverage at some earlier time $\sigma(t_0)$. We take $t_0=3$ h, use $w=0.008$ nm^3, $\nu=3/a^2$ (with $a=0.76$ nm), and $N=625$, and the coverage data from Table II to plot the evolution of surface coverage as a function of time (Fig. 7). The gradient of 1.3×10^{-4} chains/nm^2/s is 20 times smaller than the calculated value of $(c_0\nu k_BT/24\eta N)$. This implies that the coverage is increasing more slowly than predicted by the SCF model for the kinetics we outline in the Appendix.

We should point out that our kinetic model neglects the effects of desorption and assumes the bulk concentration remains constant. We believe both these assumptions to be valid until the system is very close to equilibrium: the potential well occupied by surface attached molecules is about $27k_BT$ (assuming the sticking energy to be three times that of a chain bearing a single zwitterion); this means that the rate of desorption will be negligible until equilibrium is reached (at which point, the rate of adsorption will be similarly negligible).

We should also emphasize that both the scaling and SCF descriptions of the potential barrier are *mean-field* treatments. As such they take no account of local inhomogeneities in the monomer density in the brush environment. Physically one might expect there to be inhomogeneities that persist on a range of time scales. Both scaling and the analytical SCF approaches are based on the assumption that the chains are strongly stretched, which will have the effect of suppressing short time-scale *fluctuations*. In a physical brush, one can imagine a variety of molecular conformations (mushroom, stretched, strongly stretched) and thermal fluc-

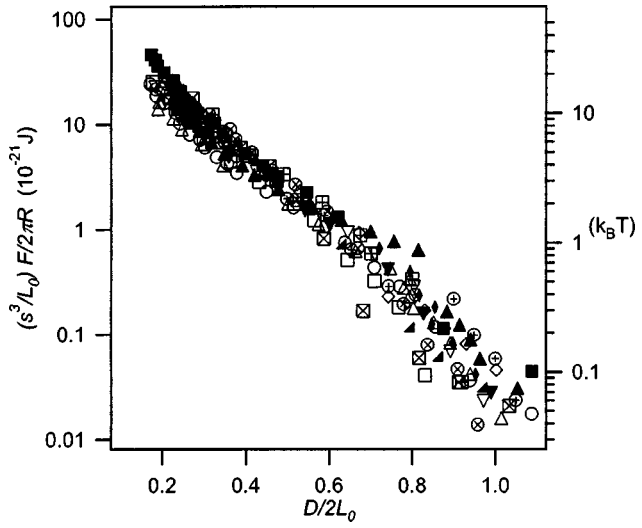

FIG. 8. Force profiles from Fig. 3(b), scaled by $s^3/2\pi L_0$, plotted as a function of $D/2L_0$; s is the average end-group spacing and L_0 the brush height. Scaling the interaction free energy in this way is equivalent to the excess free energy per blob, which we show in units of k_BT on the right-hand axis. The fact that all profiles collapse onto a single curve, provides some evidence that the brush is growing homogeneously.

tuations leading to the interconversion between these conformations. The microscopic model of Himmelhaus *et al.*[29] attempts to account for these effects by constructing an effective Hamiltonian, that allows for molecules in the brush to adopt a variety of conformations and for thermal fluctuations to allow interconversion between these conformations.

On longer time scales, one can imagine that before equilibrium is reached, the brush need not necessarily be laterally homogenous. Such nonequilibrium effects might be especially relevant in this system, as the high sticking energy will slow down surface diffusion of attached chains. The chains might be more inclined to ''stick where they hit'' which could lead to lateral inhomogeneities in the surface coverage. Laterally inhomogeneous layers of tethered polymers have been observed to form from a poor solvent.[37,38]

As the Alexander-de Gennes expression for the interaction free energy [Eq. (8)] is based on the assumption of uniform noninterpenetrating brushes, we can look for evidence of inhomogeneity in the force profiles measured for the growing brushes. In Fig. 8 we show the data from Fig. 3(b), replotted as the interaction free energy scaled by the appropriate value of s^3/L_0, where s is the average anchor spacing and L_0 the brush height, as a function of $D/2L_0$. The fact that all the profiles collapse onto a single curve suggests that the Alexander-de Gennes description [Eq. (8)] is appropriate for the growing brush and that the force profiles provide no evidence for inhomogeneous brush growth. We note that Kelley *et al.* have observed heterogeneity in polystyrene brushes formed from diblock copolymers and comment that interactions between surfaces bearing such layers also scale in the manner expected for uniform brushes.[39] However, we again comment that direct correlation of surface structure and interactions for brushes formed from diblocks may be complicated by interactions within the layer formed by the sticking block.[34]

In the Appendix we show that the flux of molecules incident on the surface can be described as the product of the concentration of molecules that have sufficient energy to surmount the barrier (Boltzmann population) multiplied by the velocity of crossing the barrier. In reality, the end group occupies a finite area, so to obtain a measure of the rate of sticking, this incident flux should be multiplied by the probability that the end group lands on an empty site. Penn *et al.*[23] incorporate the effect of inhomogeneity by using the phenomenological cooperative sequential adsorption (CSA) model. They model the tethering kinetics using a Monte Carlo approach in which each polymer chain is represented by a disk of radius R_g in the relaxed state. The probability of adding a polymer chain is taken to be the product of the probability of penetrating the barrier presented by the already attached polymers (as in the SCF and scaling treatments) *and* a second probability that was determined by the energy required to change the conformation of the incoming chain and the tethered chains local to the incoming chain. We do not explicitly take inhomogeneity into account but a phenomenological approach to allow for the fact that, to end-attach, an incoming chain must land on an empty site is to assume a simple Langmuir model in which the probability of striking an empty site is assumed to be $(1-\theta)$, where θ is the fractional surface coverage. In Table II we express the coverage as a fractional coverage, $\theta=\sigma/\sigma_{eq}$ where we calculate $\sigma_{eq}=0.0625$ chains/m^2 on the basis of scaling arguments. The fractional coverages of 0.79 and 0.91 at 37 and 133 h imply empty-site probabilities of 0.21 and 0.09, respectively; this would reduce the sticking flux at 133 h to 9% of that assumed in our mean-field models.

Taken together, the results of the SCF and scaling analyses of the kinetics provide qualitative support for the kinetic barrier being associated with the stretching energy of a chain as it penetrates the already present brush layer; they also indicate that the kinetics of brush formation is strongly dependent on the nature of the potential presented by the existing brush. The agreement with the self-consistent mean-field model is to within an order of magnitude and simple considerations of the physical effects not included in the model suggest how the agreement might be improved.

V. SUMMARY

We previously reported that increasing the number of zwitterionic sticking groups at the end of PS–X chains resulted in no measurable change in the surface coverage.[10] We suggested that either increasing the number of zwitterionic groups was not increasing the sticking energy (due to multipole formation) or that the kinetic effects might be playing a role.

We are now able to offer an explanation for this unexpected observation: it is a kinetic effect. We find that longer chains ($M_n=65\,000$) functionalized with three zwitterionic groups [PS(65)–X_3] will displace shorter chains ($M_n=25\,000$) bearing only one zwitterionic group [PS(25)–X] from preformed brushes. A simple consideration of the free energy of the brush indicates that this can only happen if the longer chain has a higher end-group sticking energy. This

clearly establishes that increasing the number of zwitterionic groups at the end of the polystyrene chain does increase the sticking energy of the end group.

We find that assembling $PS(65)-X_3$ onto a bare mica surface does result in a higher surface coverage than previously observed[5,10] but that the increase in coverage occurs on a much slower time scale. We suggest that the very slow increase in surface coverage with time provides an explanation for the observation that surface coverage appears to be largely independent of the supposed sticking energy of the end group:[9] the denser brushes that should result from a higher sticking energy are kinetically limited; Habicht *et al.* reach the same conclusion and suggest that the grafting from approach provides a better strategy to achieve dense brushes.[40]

We use refractive index measurements to provide a direct measure of the surface coverage for the growing brush. Comparison with mean-field models for the kinetics of brush growth provides qualitative support for associating the kinetic barrier with the stretching of an incoming chain that is required if the chain is to penetrate the existing brush and attach to the surface. Phenomenological considerations allow us to make suggestions of how these models could be improved. The dominant contribution to the potential barrier is the excluded volume (osmotic) contribution. This suggests that strategies to produce high density brushes using the grafting to approach should seek to decrease this contribution: this immediately suggests reducing the solvent quality or end-attaching from a melt. Consideration of our model for the kinetics suggests that these strategies may not be without problems: in a poor solvent the tails will be collapsed on the surface, decreasing the probability that the sticky group lands on an empty site; in grafting from a melt the ''solvent'' viscosity will be high, decreasing the reptative mobility of incoming chains.

ACKNOWLEDGMENTS

The authors gratefully acknowledge: the Royal Society for a URF (ST); the EPSRC for a PDRA (WHB), a studentship (IED) and an equipment grant; the technical expertise of the Mechanical and Electronic Workshops of the PTCL.

APPENDIX A: SCF FORMALISM—CHEMICAL POTENTIAL AND ADSORPTION ISOTHERM

The end-functionalized chain (zwitterionic end group $+$PS tail) will only experience an attraction to the surface when the zwitterionic end-group approaches to within δ of the surface, where δ is the range of the dipole-induced-dipole interaction. At greater distances from the surface, the chemical potential of the chain will be dominated by the chemical potential of the PS tail in the brush environment. It is this chemical potential which determines the dynamics of a chain in the brush and consequently the kinetics of brush formation and the equilibrium structure of the brush. As this chemical potential plays a key role in interpreting both the equilibrium structure and the kinetics of brush formation, we present here, in outline, a derivation of the chemical potential of a chain in the brush environment based on the original treatments of Milner and co-workers.[41,42] The aim is not to provide new results but rather to construct the result in a form that is appropriate for direct comparison with our experimental data.

To permit unambiguous comparison with our experimental data, we start from Milner's result[42] for the free energy per unit area of the uncompressed brush that he uses for direct comparison with the experimental force profiles of Taunton:[5]

$$\frac{f_0}{k_BT}=\left(\frac{9}{10}\right)\left(\frac{\pi^2}{12}\right)^{1/3}N\sigma^{5/3}w^{2/3}\nu^{1/3}. \tag{A1}$$

In this expression, and the following, w is the excluded volume parameter, ν has dimensions of $(\text{length})^{-2}$ and is defined by the partition function of the system, σ is the number of chains per unit area and N is the number of monomers in the chain. Milner uses the partition function to determine values for ν and w from experimental measurements of the end-to-end distance ($R_e^2=6R_g^2=3N/\nu=Na^2$) and osmotic pressure of chains in solution at a comparable concentration to that found in the experimental brushes: this procedure yields $w^{1/3}=0.2$ nm and $(3/\nu)=a^2=(0.76\ \text{nm})^2$, where a is the segment length.[42]

Assume the brush occupies an area $\mathcal{A}$ so that the free energy of the tails in the brush $\mathcal{F}_{\text{tails}}=\mathcal{A}f_0$ and the number of chains in the brush $n=\sigma\mathcal{A}$, the chemical potential of the chain in the brush at a distance just greater than δ from the surface can be determined as

$$\begin{aligned}\frac{\mu_{\text{tail}}}{k_BT}&=\frac{1}{k_BT}\left(\frac{\partial\mathcal{F}_{\text{tails}}}{\partial n}\right)_{\mathcal{A}}\\&=\frac{1}{k_BT}\left(\frac{\partial f_0}{\partial\sigma}\right)_{\mathcal{A}}=\frac{3}{2}\left(\frac{\pi^2}{12}\right)^{1/3}N\sigma^{2/3}w^{2/3}\nu^{1/3}.\end{aligned} \tag{A2}$$

Clearly the chemical potential at the bottom of the brush can be equated with the maximum in the effective potential experienced by an incoming chain (see Fig. 7), $\mu_{\text{tail}}/k_BT=U^*$; in Appendix B we show the key role this potential barrier plays in determining the kinetics of chain adsorption.

When an incoming chain has surmounted this barrier, it falls into the potential well, associated with the attraction of the zwitterionic end group for the surface, lowering its total energy to $(U^*-\Delta)k_BT$. Imagining the surface as a checkerboard lattice, it is clear that at a coverage below saturation, there will be an entropic contribution to the free energy of an end-adsorbed chain: the area occupied by one chain is σ^{-1}; unit area is ν^{-1}, hence $S_{\text{chain}}=k_B\ln(\sigma^{-1}\nu)=-k_B\ln(\sigma a^2/3)$. The free energy of a single, end-adsorbed chain, in the brush is

$$\frac{f}{k_BT}=U-TS=(U^*-\Delta+\ln|\sigma a^2/3|). \tag{A3}$$

Hence the free energy of the brush covering an area, $\mathcal{A}$, is

$$\frac{\mathcal{F}_{\text{brush}}}{k_BT}=n(U^*-\Delta+\ln|(n/\mathcal{A})a^2/3|). \tag{A4}$$

Consequently, the chemical potential of an end-adsorbed chain in the brush can be determined as

$$\frac{\mu_{\text{brush}}}{k_BT}=\frac{1}{k_BT}\left(\frac{\partial \mathcal{F}_{\text{brush}}}{\partial n}\right)_{\mathcal{A}}=(-\Delta+U^*+\ln|\sigma a^2/3|+1). \tag{A5}$$

For dilute bulk solutions (volume fraction ϕ_b), such as those used to incubate the surfaces in the experiments described in this paper, the chemical potential of a chain in the bulk may be approximated by $\mu_{\text{bulk}}\cong k_BT\ln\phi_b$.

At equilibrium, the chemical potentials of a chain in the bulk and end-adsorbed in the brush will be equal, giving the following expression for the adsorption isotherm:

$$\phi_b=(\sigma a^2/3)\exp(-\Delta+U^*). \tag{A6}$$

This result is equivalent to that of Ligoure and Leibler[12] but has been developed in a form that allows consistent comparison with our experimental data.

APPENDIX B: KINETICS OF BRUSH FORMATION—EFFECT OF THE SHAPE OF THE POTENTIAL

Here we adopt the approach originally employed by Halperin[43] and subsequently followed by Johner and Joanny,[20] and Ligourre and Leibler.[12] As with Appendix A, our intention is not to provide a new model, but rather to develop the existing models in a transparent framework that can easily and consistently be applied to the experimental data presented in the main body of the paper.

At the heart of the approach is a diffusion-convection equation for the flux of chains inside the brush:

$$J=-D(z)\left[\frac{\partial c}{\partial z}+c\frac{\partial U}{\partial z}\right] \tag{B1}$$

in which, c is the concentration of chains (chains/unit volume), U is the potential experienced by the chain at a distance z from the surface, and $D(z)$ is the appropriate diffusion coefficient for a chain approaching the surface through the existing brush environment. Equation (B1) can be recast as

$$\frac{-J}{D(z)}=\exp[-U(z)]\frac{\partial\{c\exp[U(z)]\}}{\partial z}, \tag{B2}$$

which if the flux is constant through the brush can be integrated to give

$$J=-\frac{(c_0-c_s)}{\int_0^{L_0}\frac{\exp[U(z)]}{D(z)}dz}, \tag{B3}$$

where c_s is the concentration that would be in equilibrium with the surface coverage σ. We show below that the increase in the surface coverage is sensitive to the form of the potential $U(z)$.

1. Scaling approach

We first follow the approach of Johner and Joanny[20] who employ a scaling theory description of the energetics of a chain in the brush environment, $U(z)=F(z)/k_BT$, with $F(z)$ given by Eq. (B4):

$$F(z)=k_BT\sigma^{1/2}(L_0-z). \tag{B4}$$

This potential is illustrated schematically in Fig. 6: the free energy cost (in k_BT) of a chain at a distance z from the surface is equal to the number of blobs that have been inserted into the brush of height L_0; in the scaling approach blobs have a constant size ($\sigma^{-1/2}$) and each blob has an energetic cost k_BT. That part of the incoming chain already inserted into the brush is assumed to diffuse in a reptative fashion, hence the mobility Λ is given by

$$\Lambda^{-1}=6\pi\eta(L_0-z). \tag{B5}$$

Using the Einstein relation gives the appropriate diffusion coefficient as

$$D(z)=\frac{k_BT}{6\pi\eta(L_0-z)}. \tag{B6}$$

In the language of Kramer's rate theory, the denominator of Eq. (B3) is the reciprocal of the transparence (K^{-1}):

$$K^{-1}=\int_0^{L_0}\frac{\exp[U(z)]}{D(z)}dz=\frac{6\pi\eta}{k_BT}\int_0^{L_0}(L_0-z)\exp[\sigma^{1/2}(L_0-z)]dz. \tag{B7}$$

This can be easily integrated:

$$K^{-1}=\frac{6\pi\eta}{k_BT}\left[\frac{L_0\exp(\sigma^{1/2}L_0)}{\sigma^{-1/2}}\right]. \tag{B8}$$

Using the scaling expression for the height of the brush [Eq. (1)] gives the result of Johner and Joanny:[20]

$$J=-(c_0-c_s)\frac{k_BT(\sigma a^2)^{1/6}}{6\pi\eta Na^2}\exp[-N(\sigma a^2)^{5/6}]. \tag{B9}$$

Conservation of chains at the adsorbing surface means this flux can be related to the rate of increase in surface coverage (σ=chains/unit area),

$$\frac{d\sigma}{dt}=-J|_{\text{surface}}. \tag{B10}$$

It is important to note that this treatment applies to chains approaching well covered surfaces and does not describe the initial diffusion limited adsorption of chains into the mushroom regime, which is fast on the time scale of the experiments reported here. When the system is still far from equilibrium, c_s may be set to zero: the barrier to adsorption is sufficiently large that the effects of saturation are only important close to equilibrium which is approached very slowly.

Combining Eqs. (B9) and (B10) gives a first-order differential equation, which can be integrated to give the surface coverage as a function of time:

$$(\sigma a^2)^{5/6}=\mathcal{C}+N^{-1}\ln\left|\frac{t}{\tau}\right| \tag{B11}$$

where $\tau=6\pi\eta/c_0k_BT$ is the characteristic time for brush growth.

2. SCF approach: Influence of asymmetric potential

If the SCF description of the brush the brush is adopted, the shape of the potential experienced by an incoming chain changes from Figs. 6 to 7, as derived explicitly by Milner.[35] It is important to point out the inadequacy of the schematic representation in Fig. 7: z^* is comparable with δ, the length scale over which the dipole-induced-dipole interaction between the zwitterion and the surface is significant, i.e., $z^* \sim 1$ nm; by contrast the brushes measured in this study have height, $L_0 \sim 40-55$ nm; the potential is very *asymmetric*.

In the preceding section we considered inserting chains into a potential which increased linearly as z^* was approached from the solution side. This corresponds to a constant blob size and monomer density within the brush. Consequently, inserting one additional blob (energy penalty k_BT) advances the chain by the same positional increment Δz, independent of how far into the brush the chain has penetrated. In the SCF description, the monomer concentration follows a parabolic profile. In terms of blobs containing a constant number of monomers, the blob size is decreasing as the distance from the surface decreases. By keeping the number of monomers/blob constant we can still associate a free energy penalty of k_BT with the insertion of an additional blob (i.e., the insertion of n_b more monomers into the brush environment). However, the distance that the chain advances in return for paying the free energy toll decreases: the potential gradient increases; this qualitative picture is consistent with Milner's potential illustrated in Fig. 7. The simple form of the scaling potential permitted direct integration of Eq. (B3), taking explicit account of the position dependent potential and mobility. This is more difficult for the more complex SCF potential so we adopt a different approach.

a. Case I: Symmetric potential

To gain some insight into the problem, we apply the approach outlined by Halperin[43] to a potential which is symmetric about z^*:

$$U^{\mathrm{sym}} = U^* - \omega(z-z^*)^2/2. \tag{B12}$$

Equation (B3) becomes

$$J = -\frac{c_0}{\exp(U^*)\displaystyle\int_0^{L_0} \frac{\exp[-\omega(z-z^*)^2/2]}{D(z)}\,dz}. \tag{B13}$$

The position-dependent diffusion coefficient $[D(z)]$ will smallest at z^*, hence the main contribution to the integral will be from the range around z^*. To take this into account we replace the upper limit on the integral by ∞ and $D(z) = D(z^*)$. From Eq. (B12) we may associate the width of the potential k_BT below U^* with $\alpha = \sqrt{2/\omega}$. The integral over the gaussian equals $1/2\sqrt{2\pi/\omega} \approx \alpha$ and Eq. (B13) becomes

$$J = -\frac{D(z^*)c_0 \exp(-U^*)}{\alpha} = c_0 \exp(-U^*) v_{\mathrm{barrier}}, \tag{B14}$$

which has a simple physical interpretation as the concentration of chains at the top of the barrier multiplied by the velocity at which chains cross the barrier. The velocity of crossing the barrier can be defined in terms of the chain mobility at the barrier, which from Eq. (B5) is $\Lambda(z^*) = [6\pi\eta(L_0 - z^*)]^{-1}$. The chain velocity is then

$$v_{\mathrm{barrier}} = -k_BT\Lambda(z^*)\left[\frac{\partial U(z)}{\partial z}\right]_{\mathrm{barrier}}, \tag{B15}$$

where the potential gradient is the repulsive force acting on a chain approaching from the solution. For the scaling potential [Eq. (B4)] we obtain

$$v_{\mathrm{barrier}} = \frac{k_BT\sigma^{1/2}}{6\pi\eta L_0}, \tag{B16}$$

which gives the same expression for the flux as we obtained above [Eq. (B9)].

b. Case II: Asymmetric potential

We now apply this approach to the asymmetric potential illustrated schematically in Fig. 7. We use Milner's expression for the potential[35] but use Eq. (A1), which is also due to Milner,[42] to obtain a modified expression for the free energy per chain which is consistent with our comparison with experiment:

$$U(z) = \frac{2f}{\pi}\left\{\cos^{-1}\left(\frac{z}{L_0}\right) - \left(\frac{z}{L_0}\right)\left[1 - \left(\frac{z}{L_0}\right)^2\right]^{1/2}\right\}, \tag{B17}$$

where $f = 3/2(\pi^2/12)^{1/3} N\sigma^{2/3} w^{2/3} \nu^{1/3}$ is the free energy per chain in units of k_BT. Differentiating, multiplying by the mobility and substituting $L_0 = (12/\pi^2)^{2/3} N\sigma^{1/3} w^{2/3} \nu^{-1/3}$, from Ref. 42 gives the velocity of crossing the barrier as

$$v_{\mathrm{barrier}} = \frac{\nu k_BT}{24\eta N} \tag{B18}$$

which, for PS(65) ($N = 625$) in toluene ($\eta = 0.6 \times 10^{-3}$ Pa s), is $v_{\mathrm{barrier}} \sim 3 \times 10^{-3}$ ms^{-1}. For a bulk concentration of 10^{18} chains/m^2 (corresponding to $\phi_b \sim 10^{-4}$) the flux incident on the surface, $J_0 \sim 10^{15} \exp(-U^*)$ chains/m^2/s.

Conservation of flux at the surface gives the equation for the rate of increase in surface coverage:

$$\frac{d\sigma}{dt} = \frac{\nu k_BT}{24\eta N} c_0 \exp(-U^*), \tag{B19}$$

where the potential barrier, $U^* = 3/2(\pi^2/12)^{1/3} N\sigma^{2/3} w^{2/3} \nu^{1/3}$ [Eq. (A2)]. Integrating Eq. (B19) gives the following time dependence for the surface coverage:

$$\frac{3}{2B}\{\sigma(t)^{1/3}\exp[B\sigma(t)^{2/3}] - \sigma(t_0)^{1/3}\exp[B\sigma(t_0)^{2/3}]\} = \frac{c_0\nu k_BT}{24\eta N}(t - t_0), \tag{B20}$$

where $B = (3/2)(\pi^2/12)^{1/3} N w^{2/3} \nu^{1/3}$.

[1] J. Klein, Annu. Rev. Mater. Sci. **26**, 581 (1996).
[2] S. T. Milner, Science **251**, 905 (1991).
[3] A. Halperin, M. Tirrell, and T. P. Lodge, Adv. Polym. Sci. **100**, 31 (1992).
[4] E. P. K. Currie, W. Norde, and M. A. Cohen Stuart, Adv. Colloid Interface Sci. **100–102**, 205 (2003).

[5] H. J. Taunton, C. Toprakcioglu, L. J. Fetters, and J. Klein, Macromolecules **23**, 571 (1990).
[6] H. Watanabe and M. Tirrell, Macromolecules **26**, 6455 (1993).
[7] S. Alexander, J. Phys. (Paris) **38**, 983 (1977).
[8] P. G. de Gennes, Adv. Colloid Interface Sci. **27**, 189 (1987).
[9] M. S. Kent, Macromol. Rapid Commun. **21**, 243 (2000).
[10] I. E. Dunlop, W. Briscoe, S. Titmuss, N. Hadjichristidis, and J. Klein, Macromolecular Physics and Chemistry (to be published).
[11] E. Kumacheva, J. Klein, P. Pincus, and L. J. Fetters, Macromolecules **26**, 6477 (1993).
[12] C. Ligoure and L. Leibler, J. Phys. (Paris) **51**, 1313 (1990).
[13] J. Klein and E. Kumacheva, J. Chem. Phys. **108**, 6996 (1998).
[14] J. Israelachvili and G. E. Adams, J. Chem. Soc., Faraday Trans. 1 **74**, 975 (1978).
[15] H. K. Christenson, J. Chem. Phys. **78**, 6906 (1983).
[16] J. Klein, Y. Kamiyama, H. Yoshizawa, J. N. Israelachvili, L. J. Fetters, and P. Pincus, Macromolecules **25**, 2062 (1992).
[17] J. Klein, J. Chem. Soc., Faraday Trans. **79**, 99 (1983).
[18] Assuming a uniform segment concentration, which is valid at high compressions, the volume fraction of polymer is, $\phi(D)=2\Gamma/\rho D$, where ρ is the polymer density.
[19] Flory-Huggins expression for osmotic pressure, $\Pi(\phi(D))\propto\phi^2\cong$constant $\times(2\Gamma/\rho D)^2$; mean chain separation, $s\propto\sqrt{M/\Gamma}$.
[20] A. Johner and J. F. Joanny, Macromolecules **23**, 5299 (1990).
[21] A. N. Semenov, Macromolecules **25**, 4967 (1992).
[22] R. Hasegawa and M. Doi, Macromolecules **30**, 5490 (1997).
[23] L. S. Penn, H. Huang, M. D. Sindkhedkar, S. E. Rankin, K. Chittenden, R. P. Quirk, R. T. Mathers, and Y. Lee, Macromolecules **35**, 7054 (2002).
[24] A. Kopf, J. Baschnagel, J. Wittmer, and K. Binder, Macromolecules **29**, 1433 (1996).
[25] R. Zajac and A. Chakrabarti, Phys. Rev. E **49**, 3069 (1994).
[26] J.-F. Tassin, R. L. Siemens, W. T. Tang, G. Hadziioannou, J. D. Swalen, and B. A. Smith, J. Phys. Chem. **93**, 2105 (1989).
[27] C. J. Clarke, R. A. L. Jones, J. L. Edwards, A. S. Clough, and J. Penfold, Polymer **35**, 4065 (1994).
[28] C. Huguenard, R. Varoqui, and E. Pefferkorn, Macromolecules **24**, 2226 (1991).
[29] M. Himmelhaus, T. Bastuck, S. Tokumitsu, M. Grunze, L. Livadaru, and H. J. Kreuzer, Europhys. Lett. **64**, 378 (2003).
[30] H. Motschmann, M. Stamm, and C. Toprakcioglu, Macromolecules **24**, 3681 (1991).
[31] K. Schillén, P. M. Claesson, M. Malmsten, P. Linse, and C. Booth, J. Phys. Chem. B **101**, 4238 (1997).
[32] E. Pelletier, A. Stamouli, G. F. Belder, and G. Hadziioannou, Langmuir **13**, 1884 (1997).
[33] Z. Gao and H. D. Ouyang, ACS Symp. Ser. **532**, 70 (1993).
[34] A. N. Semenov and S. H. Anastasiadis, Macromolecules **33**, 613 (2000).
[35] S. T. Milner, Macromolecules **25**, 5487 (1992).
[36] A. Halperin and S. Alexander, Europhys. Lett. **6**, 329 (1988).
[37] A. Karim, V. V. Tsukruk, J. F. Douglas, S. K. Satija, L. J. Fetters, D. H. Reneker, and M. D. Foster, J. Phys. (Paris) **5**, 1441 (1995).
[38] A. Koutos, E. W. van der Vegte, and G. Hadziioannou, Macromolecules **32**, 1233 (1999).
[39] T. W. Kelley, P. A. Schorr, K. D. Johnson, M. Tirrell, and C. D. Frisbie, Macromolecules **31**, 4297 (1998).
[40] J. Habicht, M. Schmidt, J. Ruhe, and D. Johannsmann, Langmuir **15**, 2460 (1999).
[41] S. T. Milner, T. A. Witten, and M. E. Cates, Macromolecules **21**, 2610 (1988).
[42] S. T. Milner, Europhys. Lett. **7**, 695 (1988).
[43] A. Halperin, Europhys. Lett. **8**, 351 (1989).